

Self-Organizing GeV, Nanocoulomb, Collimated Proton Beam from Laser Foil Interaction at 7×10^{21} W/cm²

X. Q. Yan,^{1,2,4,*} H. C. Wu,¹ Z. M. Sheng,³ J. E. Chen,² and J. Meyer-ter-Vehn¹

¹Max-Planck-Institut fuer Quantenoptik, Hans-Kopfermann-Straße 1, D-85748 Garching, Germany

²State Key Laboratory of Nuclear Physics and Technology, Peking University, Beijing 100871, China

³Beijing National Laboratory for Condensed Matter Physics, Institute of Physics, CAS, Beijing 100190, China, and Department of Physics, Shanghai Jiao Tong University, Shanghai 200240, China

⁴Center for Applied Physics and Technology, Peking University, Beijing 100871, China

(Received 26 March 2009; published 23 September 2009)

We report on a self-organizing, quasistable regime of laser proton acceleration, producing 1 GeV nanocoulomb proton bunches from laser foil interaction at an intensity of 7×10^{21} W/cm². The results are obtained from 2D particle-in-cell simulations, using a circular polarized laser pulse with Gaussian transverse profile, normally incident on a planar, 500 nm thick hydrogen foil. While foil plasma driven in the wings of the driving pulse is dispersed, a stable central clump with $1-2\lambda$ diameter is forming on the axis. The stabilization is related to laser light having passed the transparent parts of the foil in the wing region and enfolding the central clump that is still opaque. Varying laser parameters, it is shown that the results are stable within certain margins and can be obtained both for protons and heavier ions such as He²⁺.

DOI: 10.1103/PhysRevLett.103.135001

PACS numbers: 52.59.-f, 52.38.Kd, 52.35.Mw

With the development of the chirped pulse amplification technique [1], ultraintense short laser pulses with a peak intensity as high as $I > 10^{21}$ W/cm² and contrast ratios in excess of 10^{10} are now available, allowing for studies of laser interaction with ultrathin targets [2]. Energetic ions can be produced by means of intense laser light interacting with thin foils. These ion beams are attracting much attention due to a wide range of potential applications covering radiograph transient processes [3], ion beam tumor therapy [4], and fast ignition of fusion cores [5]. As a rule, these applications require ion beams with low energy spread and high collimation.

Usually a linear polarized (LP) laser pulse is used which generates hot electrons due to $J \times B$ heating [6]. Ions are accelerated by means of electrostatic shock acceleration at the irradiated front side of the target and by target normal sheath acceleration (TNSA) at the rear side [7–11]. However, the proton pulses obtained in this way are far from monochromatic. Often the energy spread is 100%, and ions with the highest energy represent only a small fraction of the total flux [12]. Certain techniques can be used to decrease the energy spread [13–15], and the best results to date have yielded an energy spread of about 20% FWHM at relatively low energy (few MeV).

In the present Letter, we consider circular polarized (CP) light. As pointed out recently in a number of papers [16–20], CP laser pulses can accelerate ions very efficiently and produce sharply peaked spectra. When normally incident on plane foils, the light pressure is quasistationary, following only the time dependence of the pulse envelope. Electrons are then smoothly pushed into the high-density material without strong heating and ions are taken along by

means of the charge separation field. This is in contrast to linear polarization which triggers fast longitudinal electron oscillations and excessive heating.

For appropriate parameters, CP pulses may accelerate foils as a whole with most of the transferred energy carried by ions. The basic dynamics are well described by a one-dimensional (1D) phase stable acceleration model [20]. Acceleration terminates due to multidimensional effects such as transverse expansion of the accelerated ion bunch and transverse instabilities. In particular, instabilities grow in the wings of the indented foil, where light is obliquely incident and strong electron heating sets in. Eventually, this part of the foil is diluted and becomes transparent to the driving laser light [21]. The central new observation in the present Letter is that this process of foil dispersion may stop before reaching the center of the focal spot and that a relatively stable ion clump forms near the laser axis which is efficiently accelerated. The dense clump is about $1-2$ laser wavelengths in diameter. The stabilization is related to the driving laser pulse that has passed the dispersed foil in the transparent wing region and starts to encompass the opaque clump, keeping it together. Acceleration is then similar to that studied for so-called *reduced mass targets* [22], where small droplets or clusters are used as targets. In what is described below, the new configuration is self-organizing with small pieces of matter punched out of a plane foil. In this Letter, we exhibit this new regime in terms of two-dimensional particle-in-cell (2D-PIC) simulations.

In the simulations, we have taken a CP laser pulse with wavelength $\lambda = 1 \mu\text{m}$ and maximum normalized vector potential $a = eA/mc^2 = 50$, corresponding to an intensity

of $I = 1.37 \times 10^{18} \text{ W/cm}^2 2a^2/\lambda^2$. The pulse has a Gaussian radial profile with $2\sigma = 20\lambda$ full width at half maximum and a trapezoidal shape longitudinally with 20λ flat top and 1λ ramps on both sides. It is normally incident from the left on a uniform, fully ionized hydrogen foil of thickness $D = 0.5\lambda$ and normalized density $N = n_e/n_{\text{crit}} = 80$, where the electron density n_e is given in units of the critical density $n_{\text{crit}} = \pi m_e c^2/\lambda^2$ and c is the velocity of light. The proton to electron mass ratio is $m_p/m_e = 1836$. The size of the simulation box is $50\lambda \times 80\lambda$ in (x, y) directions, respectively. A wide transverse margin ($>3.5\sigma$) has been chosen to eliminate boundary effects. We take 100 particles per cell per species and a cell size of $\lambda/80$. The flat plasma foil is located at $x = 10\lambda$ initially. Periodic boundary conditions are used for particle and fields in transverse direction, and fields are absorbed at the boundaries in longitudinal direction.

The temporal evolution of the foil is shown in Fig. 1, separately for electron and ion density. One observes that electrons and ions move closely together. At $t = 16$ (in units of laser period), about 6 laser cycles after the pulse front has reached the plasma, the foil is slightly curved, following the transverse Gaussian profile of the laser pulse. At $t = 36$, a periodic structure having approximately 1λ

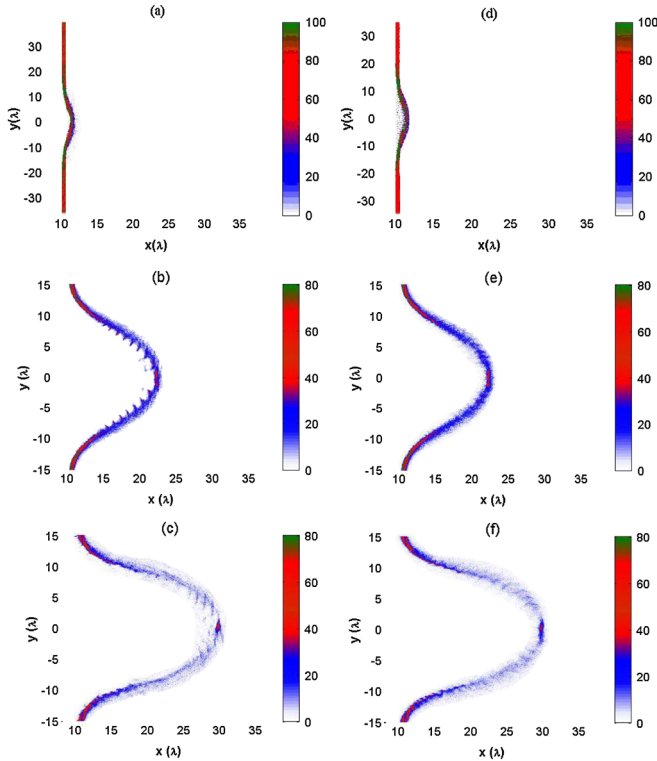


FIG. 1 (color online). Foil density evolution. Left: electrons, right: ions, at times (a),(d) $t = 16$, (b),(e) $t = 36$, (c),(f) $t = 46$, in units of laser period. The laser pulse is incident from the left and hits the plasma at $t = 10$. Only half the transverse size of the simulation box is plotted in frames (b), (c), (e), (f), for better resolution of fine structures.

scale is seen, very prominently in the electron distribution, but also already imprinted in the ion distribution. Such surface rippling has been identified before in a number of numerical studies [6,18,19,22–24] and has been described as a Rayleigh-Taylor-type instability (RTI) occurring in thin foils when driven by strong radiation pressure [25–27]. Here we depict it when the foil is already strongly deformed. At this time, the laser light is reflected from the indented walls and creates an intense standing-wave pattern at the bottom of the crater [see Fig. 2(a)].

We attribute the foil rippling to this λ -period seed pattern, at least in part. A second source is a fast current instability, setting in at early times when the foil is still plane. It has been described in [24]. Inspecting the longitudinal j_x current at time $t = 36$ in Fig. 2(c), a periodic structure of current cells can be recognized, also with λ period. It indicates a pattern of forward and backward currents typical for Weibel instability, which is known to grow fast on the time scale of the inverse plasma frequency ω_p^{-1} , which is shorter than the light period for solid density. These current patterns contribute to the unstable foil dynamics in the wing region.

Another important aspect is that the foil is strongly accelerated as a whole, and RTI depending on ion motion will add to perforate and break the foil. This is clearly seen in Figs. 1(c) and 1(f), both for electrons and ions. Using the RTI growth rates derived in [26], we find e folding within 6 laser cycles for the wing region which is consistent with the present simulation. The actual dynamics are very complicated, combining RTI and Weibel instabilities in the phase of nonlinear evolution. This is not yet understood in detail and needs separate investigation. As a result, the foil

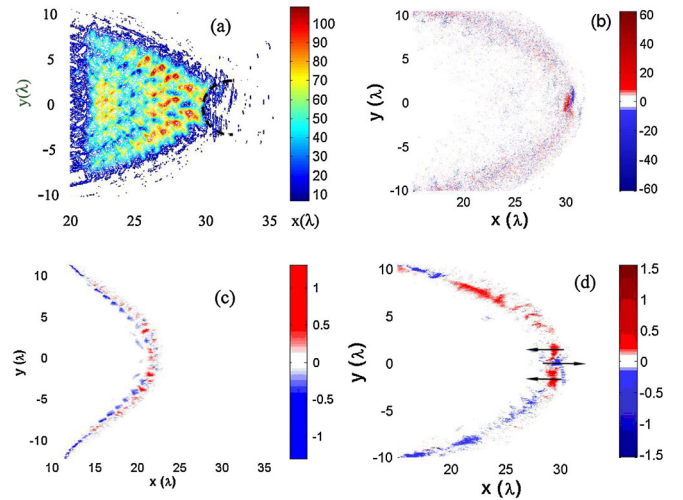


FIG. 2 (color online). (a) Laser field $\sqrt{E_y^2 + E_z^2}$ at $t = 46$, the dashed line marks the concave pulse front pushing the ion clump; (b) charge density distribution $(n_i - n_e)$ at $t = 46$; (c) current density at $t = 36$ (normalized by $en_e c$); (d) current density at $t = 46$. The black arrows in the clump region indicate the direction of electron motion.

becomes transparent in the wing region, where then light starts to pass the foil and to overtake the dense clump located near the laser axis [see Fig. 2(a)].

Let us now describe the evolution of the central clump in more detail. From Figs. 1(c) and 1(f) we see that the transverse extension of the clump is about 2λ at $t = 46$. On these small scales, only a microscopic treatment as in a PIC simulation can describe the dynamics adequately. In Fig. 2(a) it indicates that the laser pulse enfolds the clump and tends to keep it together. Plotting charge density ($n_i - n_e$) in Fig. 2(b), one recognizes how electrons [blue (dark gray)] are running ahead dragging ions [red (medium gray)]. Here the deviation from axial symmetry reflects the fact that the laser electric field is not axially symmetric, but rotates with the laser frequency. S. Rykovanov has documented the corresponding spiralling electron motion in movies [17].

The current cells, seen with λ period at time $t = 36$ in Fig. 2(c), have almost been dissolved at time $t = 46$ in Fig. 2(d), except for the central cell on the laser axis which is stabilized by the local laser field. The black arrows in Fig. 2(d) indicate the electron motion around the clump. Electrons move in the laser's direction on the axis and return on the side of the clump. The central plasma current generates at $|y| = \lambda$ a magnetic field of more than a megagauss that is able to stabilize the clump by magnetic compression. Unfortunately, we did not succeed in resolving the B field separately because of the strong laser field superimposed.

Figure 3 highlights the central results concerning clump evolution. The total number of protons, located within a λ distance from the laser axis, is shown in Fig. 3(a). Because

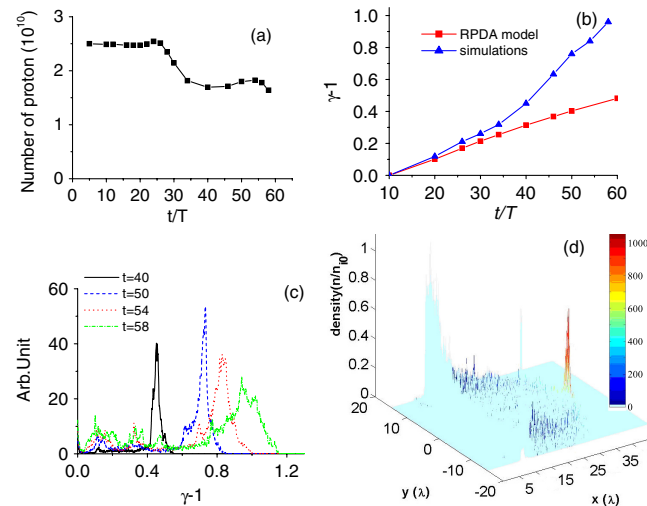


FIG. 3 (color online). (a) Number of protons in the center of the foil ($r \leq \lambda$) versus time in units of laser cycles; (b) proton energy; (c) evolution of energy spectrum for beam ions located inside the central clump ($r \leq \lambda$); (d) density and energy distributions of protons at $t = 58$ (the color bar gives ion energy in MeV).

of transverse expansion, it drops from an initial value of 2.5×10^{10} after time $t = 26$, but this trend is interrupted at about $t = 35$, when the foil becomes transparent in the wing region and the new regime of quasistable acceleration sets in. In the present 2D-PIC simulation, about 1.7×10^{10} protons (1 nanocoulomb) are trapped in the clump [see Fig. 3(a)] and are accelerated to an ion energy of approximately 1 GeV. An enhanced acceleration mode sets in at $t = 35$ after clump formation. Corresponding proton energies shown in Fig. 3(b) exceed the predictions of the radiation pressure driven acceleration (RPDA) [28] by a factor 2. At the same time, the ion energy spectra start to exhibit sharp peaks, as it is seen in Fig. 3(c). The perspective view in Fig. 3(d) then shows ion density in the (x, y) plane with color marking ion energy. One observes the high-density region of the unperturbed foil at the boundaries, the low-density plasma remains of the foil in the wing region [dark blue (dark gray)], and the accelerated ion clump sticking out as a conspicuous red (medium gray) spike in the center.

We have varied single parameters, keeping the others constant, to check the robustness of the present results. In Fig. 4(a) one observes that proton energy is rising almost linearly with laser amplitude a , while charge remains nearly constant. In Fig. 4(c) the same plot is shown for He^{2+} ions instead of protons. Figure 4(b) exhibits energy and charge as a function of laser spot size. Most important is Fig. 4(d) showing the dependence on rise time of the laser pulse. Increasing the front ramp from 1 to 10 laser cycles leaves the beam charge almost invariant while proton energy falls from 1.2 GeV to 0.7 GeV. Though high contrast over 10 laser cycles is very challenging, it may be possible to be achieved. Much progress has been made

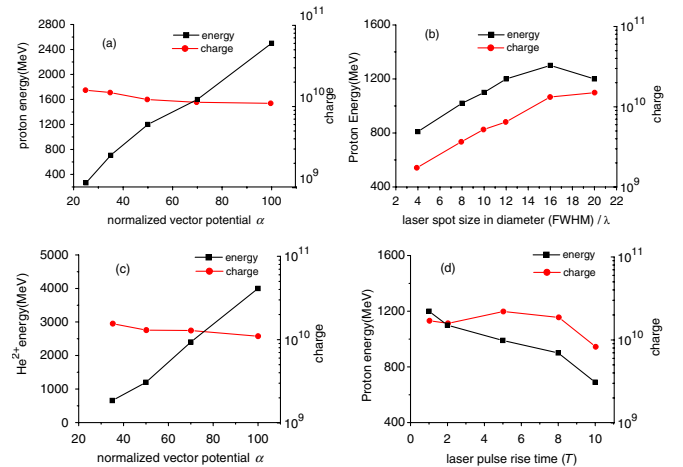


FIG. 4 (color online). Scaling studies (scan a parameter and all other parameters are fixed) (a) scaling the proton energy/charge with the normalized vector potential a ; (b) proton energy/charge with the laser spot size; (c) scaling the helium energy/charge with a ; (d) Proton energy/charge with the rise time in the unit of laser cycles.

recently in generating laser pulses with ultrahigh contrast [29].

In summary, we have identified a new regime of laser ion acceleration and have described the essential dynamics, self-organizing a mass-limited ion clump which is accelerated in a quasistable manner over many laser cycles without dispersion. This leads to sharply peaked proton spectra with energies of 1 GeV and more. The scaling studies demonstrate that the self-organizing mechanism is robust not only for hydrogen plasma, but also for heavier ion species. These findings, obtained on the basis of multi-dimensional PIC simulations, go beyond results on phase stable acceleration published so far. An important point is that the nonlinear physics itself selects the amount of accelerated ions (about 1 nanocoulomb of protons in the present simulations), rather than relying on complicated target structures. This opens an option to use simple targets adequate for high-repetition rates by means of plane foils. This is attractive for applications.

One of the authors (X. Q. Y.) would like to thank the Alexander von Humboldt Foundation for financial support. This work was partially supported by NSFC (10855001, 10935002), by the Munich Centre for Advanced Photonics (MAP), and by the Association EURATOM—Max-Planck-Institute for Plasma Physics. Z. M. S. is supported in part by the National Nature Science Foundation of China (Grants No. 10674175, No. 60621063). The authors acknowledge stimulating discussions with Professor H. Ruhl and also with Dr. M. Chen and Professor A. Pukhov.

*On leave from Peking University.
xyan@mpq.mpg.de

- [1] G. A. Mourou, T. Tajima, and S. V. Bulanov, *Rev. Mod. Phys.* **78**, 309 (2006).
- [2] A. J. Mackinnon, Y. Sentoku, P. K. Patel, D. W. Price, S. P. Hatchett, M. H. Key, C. Andersen, R. A. Snavely, and R. R. Freeman, *Phys. Rev. Lett.* **88**, 215006 (2002).
- [3] M. Borghesi *et al.*, *Phys. Plasmas* **9**, 2214 (2002).
- [4] S. V. Bulanov, T. Zh. Esirkepov, V. S. Khoroshkov, A. V. Kuznetsov, and F. Pegoraro, *Phys. Lett. A* **299**, 240 (2002).
- [5] M. Roth *et al.*, *Phys. Rev. Lett.* **86**, 436 (2001); N. Naumova *et al.*, *Phys. Rev. Lett.* **102**, 025002 (2009).
- [6] S. C. Wilks, W. L. Kruer, M. Tabak, and A. B. Langdon, *Phys. Rev. Lett.* **69**, 1383 (1992).
- [7] E. L. Clark *et al.*, *Phys. Rev. Lett.* **85**, 1654 (2000); A. Zhidkov *et al.*, *Phys. Rev. E* **60**, 3273 (1999).
- [8] J. Denavit, *Phys. Rev. Lett.* **69**, 3052 (1992).
- [9] A. Zhidkov, M. Uesaka, A. Sasaki, and H. Daido, *Phys. Rev. Lett.* **89**, 215002 (2002); L. O. Silva, M. Marti, J. R. Davies, R. A. Fonseca, C. Ren, F. Tsung, and W. B. Mori, *Phys. Rev. Lett.* **92**, 015002 (2004); A. Maksimchuk, S. Gu, K. Flippo, D. Umstadter, and V. Y. Bychenkov, *Phys. Rev. Lett.* **84**, 4108 (2000).
- [10] P. Mora, *Phys. Rev. Lett.* **90**, 185002 (2003); T. Esirkepov, M. Yamagiwa, and T. Tajima, *Phys. Rev. Lett.* **96**, 105001 (2006).
- [11] Y. T. Li and Z. M. Sheng *et al.*, *Phys. Rev. E* **72**, 066404 (2005).
- [12] V. Malka *et al.*, *Med. Phys.* **31**, 1587 (2004).
- [13] H. Schworer *et al.*, *Nature (London)* **439**, 445 (2006).
- [14] T. Toncian *et al.*, *Science* **312**, 410 (2006).
- [15] M. Hegelich *et al.*, *Nature (London)* **439**, 441 (2006).
- [16] A. Macchi, F. Cattani, T. V. Liseykina, and F. Cornolti, *Phys. Rev. Lett.* **94**, 165003 (2005).
- [17] S. G. Rykovanov, J. Schreiber, J. Meyer-ter-Vehn, C. Bellei, A. Henig, H. C. Wu, and M. Geissler, *New J. Phys.* **10**, 113005 (2008); X. Zhang *et al.*, *Phys. Plasmas* **14**, 123108 (2007); C. S. Liu, V. K. Tripathi, and X. Shao, *AIP Conf. Proc.* **1061**, 246 (2008).
- [18] O. Klimo, J. Psikal, and J. Limpouch, and V. T. Tikhonchuk, *Phys. Rev. ST Accel. Beams* **11**, 031301 (2008).
- [19] A. P. L. Robinson, M. Zepf, S. Kar, R. G. Evans, and C. Bellei, *New J. Phys.* **10**, 013021 (2008).
- [20] X. Q. Yan *et al.*, *Phys. Rev. Lett.* **100**, 135003 (2008).
- [21] See EPAPS Document No. E-PRLTAO-103-007941 for the evolution of the electron density. For more information on EPAPS, see <http://www.aip.org/pubservs/epaps.html>.
- [22] A. Henig, D. Kiefer, M. Geissler, S. G. Rykovanov, R. Ramis, R. Hörlein, J. Osterhoff, Zs. Major, L. Veisz, S. Karsch, F. Krausz, D. Habs, and J. Schreiber, *Phys. Rev. Lett.* **102**, 095002 (2009).
- [23] A. Macchi, F. Cornolti, F. Pegoraro, T. V. Liseykina, H. Ruhl, and V. A. Vshivkov, *Phys. Rev. Lett.* **87**, 205004 (2001).
- [24] M. Chen, A. Pukhov, Z. M. Sheng, and X. Q. Yan, *Phys. Plasmas* **15**, 113103 (2008).
- [25] E. G. Gamaly, *Phys. Rev. E* **48**, 2924 (1993).
- [26] F. Pegoraro and S. V. Bulanov, *Phys. Rev. Lett.* **99**, 065002 (2007).
- [27] Y. Yin, W. Yu, M. Y. Yu, A. Lei, X. Yang, H. Xu, and V. K. Senecha, *Phys. Plasmas* **15**, 093106 (2008).
- [28] T. Esirkepov, M. Borghesi, S. V. Bulanov, G. Mourou, and T. Tajima, *Phys. Rev. Lett.* **92**, 175003 (2004).
- [29] R. Hoerlein *et al.*, *New J. Phys.* **10**, 083002 (2008).